

Optical and magneto-optical properties of ferromagnetic $\text{La}_{1-x}\text{Ba}_x\text{MnO}_3$ single crystals

This article has been downloaded from IOPscience. Please scroll down to see the full text article.

2010 J. Phys.: Condens. Matter 22 096003

(<http://iopscience.iop.org/0953-8984/22/9/096003>)

View [the table of contents for this issue](#), or go to the [journal homepage](#) for more

Download details:

IP Address: 129.252.86.83

The article was downloaded on 30/05/2010 at 07:24

Please note that [terms and conditions apply](#).

Optical and magneto-optical properties of ferromagnetic $\text{La}_{1-x}\text{Ba}_x\text{MnO}_3$ single crystals

N G Bebenin¹, N N Loshkareva^{1,4}, A A Makhnev¹,
E V Mostovshchikova¹, L V Nomerovannaya¹, E A Gan'shina²,
A N Vinogradov² and Ya M Mukovskii³

¹ Institute of Metal Physics, Ural Division of RAS, Kovalevskaya Street 18,
Ekaterinburg 620990, Russia

² Moscow State University, Moscow 119992, Russia

³ Moscow State Steel and Alloys Institute, Leninskii Prospekt 4, Moscow 119049, Russia

E-mail: loshkareva@imp.uran.ru

Received 18 November 2009, in final form 13 January 2010

Published 10 February 2010

Online at stacks.iop.org/JPhysCM/22/096003

Abstract

The optical and magneto-optical properties of ferromagnetic $\text{La}_{1-x}\text{Ba}_x\text{MnO}_3$ single crystals with $x = 0.15, 0.20$ and 0.25 are studied. The components of the permittivity tensor are obtained by spectral ellipsometry techniques and transverse Kerr effect measurements. The Kerr effect spectra depend substantially on the Ba content. The plasma frequency is estimated. In the paramagnetic semiconductor state, the small polarons contribute to conductivity in $\text{La}_{0.85}\text{Ba}_{0.15}\text{MnO}_3$, in $\text{La}_{0.75}\text{Ba}_{0.25}\text{MnO}_3$ no evidence for polarons is found even in the semiconductor state. For $\text{La}_{0.85}\text{Ba}_{0.15}\text{MnO}_3$ ($T_C = 214$ K), the metallic phase is estimated to occupy less than 1% of the total volume at $T = 190$ K. It is shown that in $\text{La}_{0.75}\text{Ba}_{0.25}\text{MnO}_3$, the energy gap vanishes and the metal–semiconductor transition occurs somewhat below T_C rather than at $T = T_C$.

(Some figures in this article are in colour only in the electronic version)

1. Introduction

Ferromagnetic lanthanum manganites $\text{La}_{1-x}\text{D}_x\text{MnO}_3$, where D = Ca, Sr, Ba, attract attention due to the colossal magnetoresistance (CMR) observed near the Curie temperature T_C , see reviews [1–5]. To understand the nature of the CMR effect one needs information on the electron energy spectrum, especially on how the spectrum is changed when the ferromagnetic-to-paramagnetic phase transition occurs. The optical properties measurements are known to be an effective tool to obtain such information. Optical and magneto-optical measurements also allow one to reveal and study the phase separation in manganites [6].

The optical experiments on parent antiferromagnetic LaMnO_3 revealed two wide absorption bands, the first of which, located at $\sim 4\text{--}5$ eV, is attributed mainly to O(2p)–Mn(3d) charge-transfer transitions and the second band,

centered at ~ 2.0 eV, is interpreted as due mainly to an intersite d–d transition [7–9]. The value of the optical gap in LaMnO_3 is about 0.4 eV at $T = 80$ K and 0.3 eV at $T = 293$ K [10].

Doping with a divalent element results in the ferromagnetic ground state if $0.1 < x < 0.5$. When $x > x_c$, where x_c is the critical concentration for the compositional metal–semiconductor transition, the crystal is in a low-resistivity metallic state below the Curie temperature. In the case of $\text{La}_{1-x}\text{Sr}_x\text{MnO}_3$ the critical concentration is 0.17 and the ferromagnetic-to-paramagnetic phase transition is second order. At $T > T_C$, the La–Sr manganites are in a high-resistivity state with $d\rho/dT < 0$ if $x < 0.25$ and $d\rho/dT > 0$ otherwise. The evolution of the spectra of $\text{La}_{1-x}\text{Sr}_x\text{MnO}_3$ single crystals under doping was studied in [11–14], the magneto-optical Kerr effect (MOKE) was investigated in [15, 16], where the MOKE spectra were found to be nearly independent of Sr content. The main result is the strong redistribution of the optical conductivity spectra

⁴ Author to whom any correspondence should be addressed.

weight from higher energies into the infrared (IR) region with increasing x . If a manganite is in the metallic state the spectrum exhibits a pronounced Drude-like component with large spectral weight [12–14].

In the case of $\text{La}_{1-x}\text{Ca}_x\text{MnO}_3$, the critical concentration is about 0.225, the metal–semiconductor transition being very sharp [17]. The magnetic transition is second order if $x < 0.25$ and first order otherwise [18]. The optical conductivity spectra were studied in [19–24], preferably, on thin films. Overall, the results are similar to those for the La–Sr manganites. The MOKE data for $\text{La}_{0.67}\text{Ca}_{0.33}\text{MnO}_3$ polycrystalline film were reported in [25].

Optical properties of $\text{La}_{1-x}\text{Ba}_x\text{MnO}_3$ manganites are little studied. We know only one publication [26] in which Raman spectra and IR transmission spectra of polycrystalline $\text{La}_{1-x}\text{Ba}_x\text{MnO}_3$ samples were reported.

The first aim of the present work is to study the optical and magneto-optical properties of ferromagnetic $\text{La}_{1-x}\text{Ba}_x\text{MnO}_3$ single crystals with $x = 0.15, 0.20$ and 0.25 . As a rule, the optical conductivity spectra were obtained by Kramers–Kronig analysis of the reflectivity data. In our work, however, we exploit the spectral ellipsometry technique in order to obtain information on permittivity without any additional mathematical manipulations.

The electronic transport in these crystals has already been investigated [27–29], so that our second aim is to reveal the connection between the optical and transport properties. We hope that this study will shed light on the mechanism of the CMR effect, not only in La–Ba manganites but also in other CMR manganites.

2. Samples preparation and characterization

The single crystals of $\text{La}_{1-x}\text{Ba}_x\text{MnO}_3$ with $x = 0.15, 0.20$, and 0.25 were grown by the floating zone method; the details have been published elsewhere [30]. The magnetic phase transition is second order, the Curie temperatures evaluated through the Arrott–Belov curves are about 214, 252, and 300 K, respectively [27–29].

The temperature dependence of resistivity, $\rho(T)$, is shown in figure 1. Well below T_C , the $x = 0.25$ crystal is in the metallic state while the $x = 0.15$ and 0.20 manganites exhibit semiconductor behavior. In the case of $\text{La}_{0.80}\text{Ba}_{0.20}\text{MnO}_3$, the increase of ρ with lowering temperature is rather weak; moreover, the crystal can be transformed into the metallic state by application of a hydrostatic pressure of about 10 kbar [31]. It follows that in the $\text{La}_{1-x}\text{Ba}_x\text{MnO}_3$ system, the critical concentration $x_c > 0.2$ and hence is close to that in $\text{La}_{1-x}\text{Ca}_x\text{MnO}_3$ family. In the paramagnetic state, all the crystals are semiconductors.

3. Optical experiments

The reflection plane was made by using diamond polishing paste. The refractive index, n , and extinction ratio, k , were measured by the ellipsometry technique at temperatures of 95, 300, and 400 K in the spectral range of 0.2–4.8 eV. The measurements were performed at an angle of incidence of

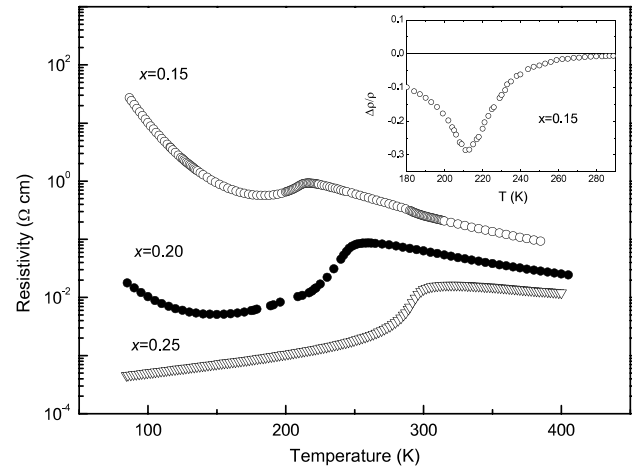


Figure 1. Temperature dependence of resistivity of $\text{La}_{1-x}\text{Ba}_x\text{MnO}_3$ single crystals (after [27–29]). Inset: magnetoresistance of $\text{La}_{0.85}\text{Ba}_{0.15}\text{MnO}_3$ measured at $H = 10$ kOe [29].

about 67° . The real part of the optical conductivity, $\sigma_{1xx}(E)$, and the real, ε_{1xx} , and imaginary, ε_{2xx} , parts of the permittivity $\varepsilon_{xx} = \varepsilon_{1xx} - i\varepsilon_{2xx}$ were calculated in accordance with the following formulae: $\sigma_{1xx}(E) = nk\omega/2\pi$, $\varepsilon_{1xx} = n^2 - k^2$, $\varepsilon_{2xx} = 2nk$. Here $E = \hbar\omega$ is the photon energy.

To study the optical spectra in the infrared (IR) region in more detail, we measured the reflection coefficient R in the spectral range of 0.04–1.2 eV using an IR spectrometer at room temperature. In addition, the absorption spectrum of $\text{La}_{0.85}\text{Ba}_{0.15}\text{MnO}_3$ was taken in the spectral range of 0.13–0.26 eV at temperatures from 200 to 245 K i.e. just below and above T_C . In the absorption measurement, a plane-parallel plate of $30 \mu\text{m}$ thick was used. We failed to study the light absorption in other La–Ba crystals because of too strong absorption.

To study the magneto-optical properties we used measurements of the transverse Kerr effect that appears as an intensity variation of the p -polarization light reflected by the sample under magnetization (the magnetic field was aligned parallel to the sample surface and perpendicular to the light incidence plane). Writing the dielectric tensor in the form

$$\tilde{\varepsilon} = \begin{Bmatrix} \varepsilon_{xx} & -i\varepsilon_{xy} & 0 \\ i\varepsilon_{xy} & \varepsilon_{xx} & 0 \\ 0 & 0 & \varepsilon_{zz} \end{Bmatrix}, \quad (1)$$

where $\varepsilon_{xx} = \varepsilon_{1xx} - i\varepsilon_{2xx}$, $\varepsilon_{xy} = \varepsilon_{1xy} - i\varepsilon_{2xy}$, we can express the variation of the reflected light intensity for the p -wave due to the magnetization of the ferromagnetic sample as follows [32]

$$\delta_p = 2 \sin 2\varphi \frac{A_1}{A_1^2 + B_1^2} \varepsilon_{1xy} + 2 \sin 2\varphi \frac{B_1}{A_1^2 + B_1^2} \varepsilon_{2xy}, \quad (2)$$

where φ is the incident angle, $A_1 = \varepsilon_{2xx}(2\varepsilon_{1xx} \cos^2 \varphi - 1)$, and $B_1 = (\varepsilon_{2xx}^2 - \varepsilon_{1xx}^2) \cos^2 \varphi + \varepsilon_{1xx} - \sin^2 \varphi$.

The measurements of MOKE were made using an automatic spectrometer. A dynamic method to record MOKE was used. The relative change in the intensity of the reflected light

$$\delta_p = [I(H) - I(0)]/I(0), \quad (3)$$

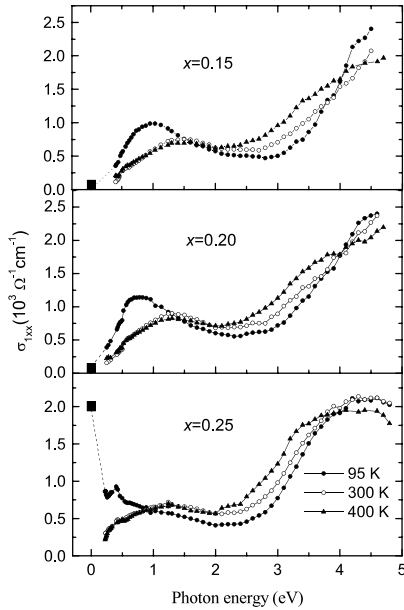


Figure 2. Optical conductivity of $\text{La}_{1-x}\text{Ba}_x\text{MnO}_3$ single crystals. Solid squares stand for dc conductivity.

where $I(H)$ and $I(0)$ are the intensities of the reflected light in the presence and in absence of a magnetic field, respectively, was directly measured in the experiment. The magnitude of the alternating magnetic field in the gap of an electromagnet was up to 3.5 kOe. The sensitivity of the apparatus was 10^{-5} . The MOKE spectra were recorded in the photon energy range of 0.5–4.3 eV at various light incidence angles.

The samples for the ellipsometric and MOKE measurements were annealed in an Ar atmosphere in order to reduce the mechanical stress created during polishing.

4. Results of ellipsometry measurements

We start with analysis of the optical conductivity because it is σ_1 that is usually considered in the articles on the optical properties of the CMR manganites.

Figure 2 shows σ_1 versus E . One can see two broad absorption bands, which are typical for the LaMnO_3 -based compounds. At $T = 300$ and 400 K, i.e. at $T \geq T_C$, the low-energy band (hereafter referred to as band 1) has maxima at $E \approx 1.5$ eV ($x = 0.15$) and $E \approx 1.3$ eV ($x = 0.20$ and 0.25). The high-energy band (band 2) occupies the region above 2.5 eV and has a maximum at $E \sim 4$ eV. Decreasing T down to 95 K results in the shift of band 1 to lower energies while the low-energy wing of band 2 moves to higher energies.

The fact that in the paramagnetic state, i.e. when the magnetization is equal to zero, band 1 remains practically unchanged while in the ferromagnetic state this band is sensitive to temperature points to the dependence of the position and intensity of this band on the total magnetization, i.e. on whether Mn spins are aligned or not. Therefore, the optical transitions responsible for band 1 involve electron states of at least two Mn ions. Recently Kovaleva *et al* [7] have shown that in the parent LaMnO_3 , band 1 is formed by intersite

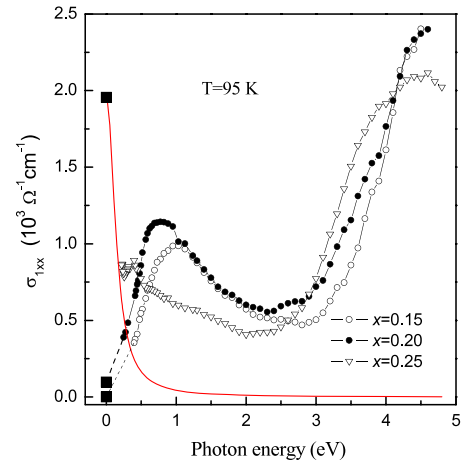


Figure 3. The evolution of optical conductivity with doping at $T = 95$ K. The solid squares stand for dc conductivity. The solid line shows the coherent contribution.

transitions across the Mott gap, i.e. transitions between e_g -states of neighboring Mn ions. Obviously, our results are consistent with such an interpretation. It is necessary to remember, however, that between two Mn ions there is an oxygen ion, therefore transitions involving oxygen states may also give a contribution to band 1; a contribution due to intrasite transitions cannot be excluded completely.

As for band 2, it is commonly accepted that this band is due to the charge-transfer transitions from 2p states of oxygen to 3d states of manganese.

The evolution of the optical conductivity spectrum with increasing Ba content in the ferromagnetic state ($T = 95$ K) is shown in figure 3. An increase of x leads to the shift of the spectrum to lower energies, which is similar to what is observed in the case of $\text{La}_{1-x}\text{Sr}_x\text{MnO}_3$ manganites [12]. The maximum of band 1, located at $E = 1.0$ eV if $x = 0.15$, is situated at $E = 0.8$ eV if $x = 0.20$. At the low-energy wing of the band 1, the optical conductivity σ_{1xx} of the $x = 0.15$ and 0.20 crystals decreases as E decreases, so that it is reasonable to think that at $E \rightarrow 0$ the optical conductivity falls down to the static conductivity $\sigma_o(T) = \rho^{-1}(T)$ at $T = 95$ K, which is equal to $0.05 \Omega^{-1} \text{cm}^{-1}$ if $x = 0.15$ and $97 \Omega^{-1} \text{cm}^{-1}$ when $x = 0.20$. In the case of the $x = 0.25$ manganite, there is a weak peculiarity at ≈ 0.4 eV on the background of the Drude-like growth of conductivity.

It is very useful to analyze not only the optical conductivity but also permittivity $\epsilon_{xx} = \epsilon_{1xx} - i\epsilon_{2xx}$. The energy dependencies of ϵ_{1xx} and ϵ_{2xx} are presented in figures 4 and 5. For $\text{La}_{0.85}\text{Ba}_{0.15}\text{MnO}_3$ and $\text{La}_{0.80}\text{Ba}_{0.20}\text{MnO}_3$, ϵ_{1xx} is positive in both the paramagnetic ($T = 300$ and 400 K) and ferromagnetic ($T = 95$ K) states, so that the free charge carrier contribution is negligible. On the contrary, in the case of $\text{La}_{0.75}\text{Ba}_{0.25}\text{MnO}_3$, the real part of the permittivity is negative below 0.6 eV, indicating the free carriers' predominance. Using the data on ϵ_{1xx} and ϵ_{2xx} one can estimate the plasma frequency, ω_p , as the frequency at which the energy-loss function $\text{Im}(1/\epsilon_{xx}) = \epsilon_{2xx}/(\epsilon_{1xx}^2 + \epsilon_{2xx}^2)$ is maximal. We have obtained $\omega_p = 2.3 \times 10^{15} \text{ s}^{-1}$ ($=1.5$ eV) at $T = 95$ K.

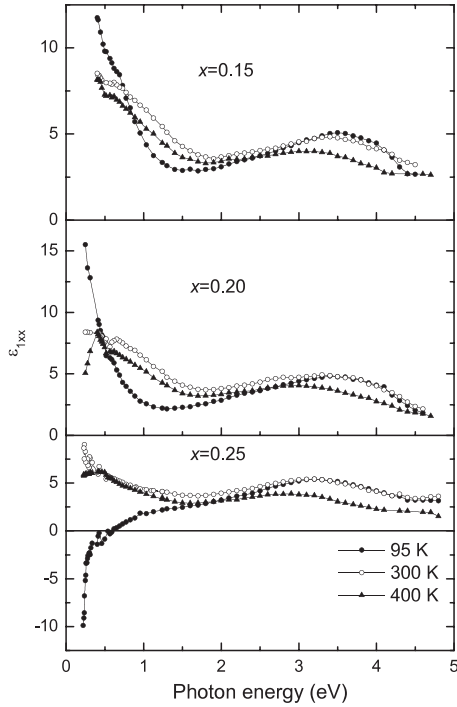


Figure 4. The ϵ_{1xx} spectra of $\text{La}_{1-x}\text{Ba}_x\text{MnO}_3$ single crystals.

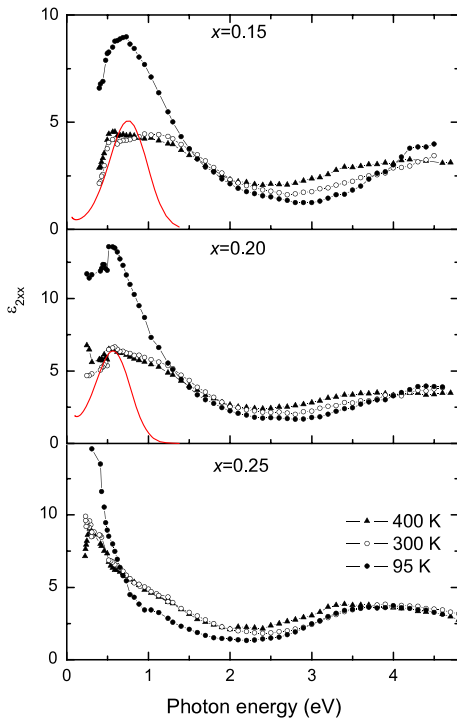


Figure 5. The ϵ_{2xx} spectra of $\text{La}_{1-x}\text{Ba}_x\text{MnO}_3$ single crystals. Solid lines are results of calculations in accordance with formulae [36, 37].

The static conductivity can be written as $\sigma_o = \omega_p^2 / (4\pi\gamma)$, where γ stands for the relaxation frequency. Thus we find $\gamma = 2.3 \times 10^{14} \text{ s}^{-1}$ and then estimate the coherent contribution to the optical conductivity for $T = 95 \text{ K}$. The result is shown in figure 3 as a solid line.

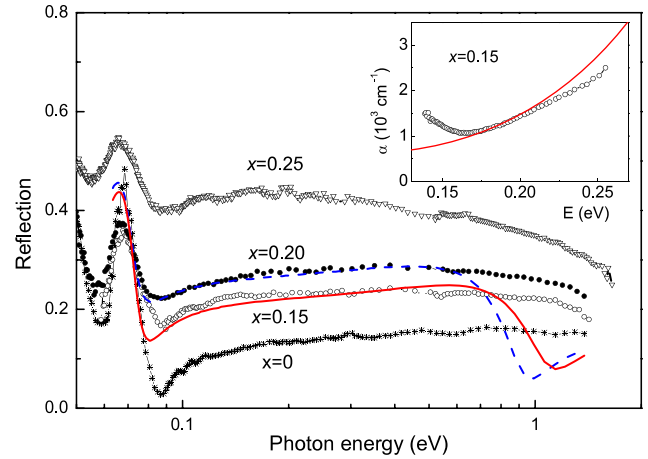


Figure 6. The reflectivity of $\text{La}_{1-x}\text{Ba}_x\text{MnO}_3$ single crystals in the infrared spectral region. Lines are results of fitting of experimental points to the polaron theory formulae [36, 37]. Inset: experimental (circles) and calculated (line) dependence of the absorption coefficient on energy.

Let us consider $\epsilon_{2xx}(E)$ in more detail. For the $x = 0.15$ and 0.20 crystals, band 1 is asymmetric, which points to its complex structure. Near the low-energy boundary, one can see a narrow band centered at about 0.6 eV . The latter was not observed in the spectrum of undoped LaMnO_3 and may thus be connected with Ba doping. The peculiarity at $\approx 0.6 \text{ eV}$ is seen at all temperatures, which suggests its position to be independent of magnetization or that such a dependence is very weak. Thus we may assume that the band around 0.6 eV is due mainly to intrasite transitions involving the electron states of a Mn^{4+} ion. A similar peculiarity was observed earlier in spectra of $\text{La}_{1-x}\text{Sr}_x\text{MnO}_3$ for $x \leq 0.125$, see [10, 11, 33].

As for the $x = 0.25$ manganite, the form of its $\epsilon_{2xx}(E)$ curves in the low-energy part of the spectra is probably caused by the shift of the aforementioned narrow band to $E \approx 0.4 \text{ eV}$ and the free charge carriers.

5. Polarons in optical spectra

In this section, we consider the optical reflection and absorption in the energy range $0.04 < E < 0.6 \text{ eV}$. Figure 6 shows the $R(E)$ curves for our La–Ba crystals taken at room temperature; the curve for LaMnO_3 is given for comparison. The phonon spectrum is situated below 0.09 eV . At $E = 0.09 \text{ eV}$, there is minimum, and in the range from 0.1 to 0.6 eV the dependence of R on energy is very weak. In the range $0.09 < E < 0.6 \text{ eV}$, the reflection coefficient is greater than the higher doping level and hence the conductivity.

The reflectivity spectra of the $\text{La}_{1-x}\text{Ba}_x\text{MnO}_3$ crystals and their evolution with doping are typical for materials in which charge carriers are of small polaron type. Thus, for instance, similar reflectivity spectra were observed in ferrites [34] and barium titanate [35]. In view of this, we tried to fit our experimental data to formulae that describe the polaron contribution to permittivity [36, 37]. The energy of the polaron hop, E_a , was our fitting parameter; the result of fitting is shown in figure 6 by lines. One can see that the fitting is satisfactory

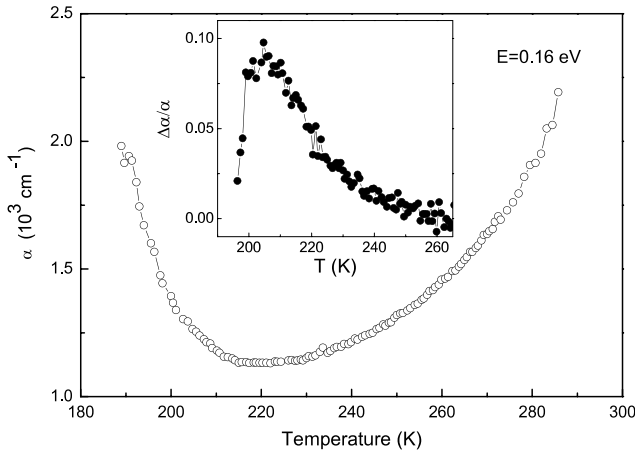


Figure 7. Temperature dependence of light absorption in $\text{La}_{0.85}\text{Ba}_{0.15}\text{MnO}_3$. Inset: the same of magneto-absorption ($H = 8$ kOe).

for the $x = 0.15$ ($E_a = 0.22$ eV) and $x = 0.20$ ($E_a = 0.17$ eV) manganites. The obtained values of E_a are somewhat greater than the activation energy $E_a^{(\rho)}$ for resistivity, which is equal to ≈ 0.13 and ≈ 0.1 eV, respectively [28, 29]. As for the $x = 0.25$ crystal, we failed to obtain a satisfactory fitting.

The calculated ε_{2xx} ($T = 300$ K) spectra are shown in figure 5 as a solid lines. One can see that the 0.6 eV band can be attributed to polarons.

As E_a is known, we can calculate the absorption coefficient $\alpha(E) = 2\omega k/c$ and compare the calculated curve with experimental data. The measurements were carried out on the thin plate of $\text{La}_{0.85}\text{Ba}_{0.15}\text{MnO}_3$ at $T = 245$ K, for at this temperature the absorption coefficient is lowest, see figure 7. The result of calculations is presented in the inset of figure 6. In the spectral range of $0.16 < E < 0.25$ eV, the calculated curve is very close to the experimental points. Notice that no additional fitting was made. Thus, we may infer that the small polarons give the main contribution to the optical properties of $\text{La}_{0.85}\text{Ba}_{0.15}\text{MnO}_3$ in the spectral range indicated.

Unfortunately we were not able to measure $\alpha(E)$ in $\text{La}_{0.80}\text{Ba}_{0.20}\text{MnO}_2$ because the light absorption was very high. Therefore we cannot say for certain that the polarons dominate permittivity; nevertheless, the good fitting of the experimental $R(E)$ spectrum suggests that this is not impossible. As for $\text{La}_{0.75}\text{Ba}_{0.25}\text{MnO}_3$, the experimental data for R cannot be described by formulae of the polaron theory [36, 37] and hence the polaron contribution to conductivity (if any) is of minor importance.

6. Phase separation and magneto-absorption

In figure 7 the absorption coefficient α of $\text{La}_{0.85}\text{Ba}_{0.15}\text{MnO}_3$ measured at $E = 0.16$ eV is plotted versus temperature. In the paramagnetic state, the decrease of T results in the increase of resistivity and the decrease of α . Below $T \approx 180$ K, the light absorption, however, increases while ρ increases. Such behavior, which was also reported for some lightly doped La–Ca and La–Sr manganites [38], indicates that small metallic droplets appear in the semiconductor matrix.

Let us estimate the volume occupied by the droplets. In the paramagnetic state, the absorption coefficient is a single-valued function of resistivity. Suppose that this is true also below T_C but for the contribution of the semiconductor matrix rather than the total absorption. For example, at $T = 190$ K (the ferromagnetic state), the resistivity $\rho = 0.577$ Ω cm and the absorption $\alpha(E = 0.16$ eV, $T = 190$ K) = 1920 cm^{-1} . At $T = 253$ K (the paramagnetic state), the resistivity is the same but $\alpha(E = 0.16$ eV, $T = 253$ K) = 1350 cm^{-1} , therefore we assume the difference $\delta\alpha = \alpha(T = 190$ K) – $\alpha(T = 253$ K) = 570 cm^{-1} to be due to the absorption in the metallic droplets. Obviously $\delta\alpha = \frac{2\pi\sigma_M}{cn} \frac{\delta V}{V}$, where σ_M is the conductivity in the metallic droplets, δV and V are the volumes of the droplets and the total volume, respectively. It is argued in [38] that σ_M is close to the minimum metallic conductivity, which is about 10^3 (Ω cm) $^{-1}$ in the CMR manganites [1]. Assuming $n = 2$, we obtain $\delta V/V \approx 0.6\%$ at $T = 190$ K.

The light absorption in the CMR manganites is influenced by a magnetic field. The inset in figure 7 shows the magneto-absorption $\frac{\Delta\alpha}{\alpha} = \frac{\alpha(H) - \alpha(0)}{\alpha(0)}$ of $\text{La}_{0.85}\text{Ba}_{0.15}\text{MnO}_3$ taken in Faraday geometry in magnetic field of 8 kOe. It is interesting to compare $\Delta\alpha/\alpha$ with the magnetoresistance $\frac{\Delta\rho}{\rho} = \frac{\rho(H) - \rho(0)}{\rho(0)}$. The inset in figure 1 shows $\Delta\rho/\rho$ measured at $H = 10$ kOe. We see that both $|\Delta\rho/\rho|$ and $\Delta\alpha/\alpha$ reach a maximum at a temperature that is a little higher than T_C but the maximum value of $|\Delta\rho/\rho|$ is almost three times greater than that of $\Delta\alpha/\alpha$. This difference indicates that a magnetic field influences the dc conductivity and the optical conductivity in different ways. It should be noted that although $\Delta\alpha/\alpha$ is not very large, the magneto-transmission, i.e. the change in intensity I of light transmitted through a plate, can be great because I is proportional to $\exp(-\alpha d)$, with d being the plate thickness [6, 25].

7. Magneto-optical Kerr effect

Experimental $\delta_p(E)$ spectra for $\text{La}_{0.85}\text{Ba}_{0.15}\text{MnO}_3$ are given for $T = 95$ and 300 K in figure 8 as a typical example. The energy dependencies of ε_{1xy} and ε_{2xy} , calculated in accordance with equation (2) for $T = 95$ K, i.e. well below Curie temperature, are shown in figure 9. One can see two bands, the first of which is centered at 1.8–2.0 eV and the second lies above 2.5 eV. The position of the first band depends weakly on doping while the second band is noticeably shifted towards lower energies with increasing x , as band 2 in the optical conductivity spectra does, see figure 3. Comparison with La–Sr manganites [15, 16] shows that in $\text{La}_{1-x}\text{Ba}_x\text{MnO}_3$ the bands are broader than in $\text{La}_{1-x}\text{Sr}_x\text{MnO}_3$ with the same x and are shifted to higher energies for $x < 0.25$, the values of ε_{1xy} and ε_{2xy} in La–Ba crystals being significantly less than in the La–Sr ones with the same doping level. Unlike in La–Sr crystals, in La–Ba manganites, the spectra of ε_{xy} depend noticeably on divalent ions content. Nevertheless the overall behavior of ε_{1xy} and ε_{2xy} in La–Ba samples at low temperatures is similar to those in La–Sr manganites, so we may assume that at $E > 2.5$ eV, the strong magneto-optical effect is due mainly to a ‘diamagnetic’ transition at $E \approx 3.5$ eV. This assumption is confirmed by the calculations in accordance with the formulae

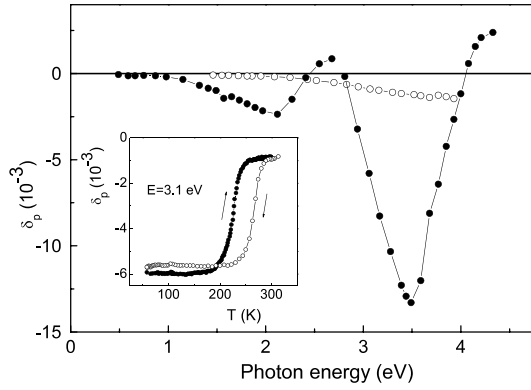


Figure 8. Transverse Kerr effect spectra of a $\text{La}_{0.85}\text{Ba}_{0.15}\text{MnO}_3$ single crystal taken in a heating run at $T = 95$ K (solid circles) and $T = 300$ K (open circles). Inset: $\delta_p(T)$ dependencies taken on heating and cooling. Incident angle $\alpha = 73^\circ$.

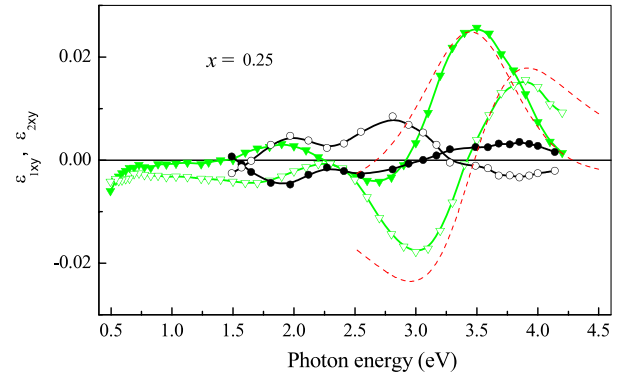


Figure 10. Energy dependence of ϵ_{1xy} (solid symbols) and ϵ_{2xy} (open symbols) of $\text{La}_{0.75}\text{Ba}_{0.25}\text{MnO}_3$ single crystals at $T = 95$ K (circles) and $T = 300$ K (triangles). Dashed lines are results of calculations with $E = 3.48$ eV.

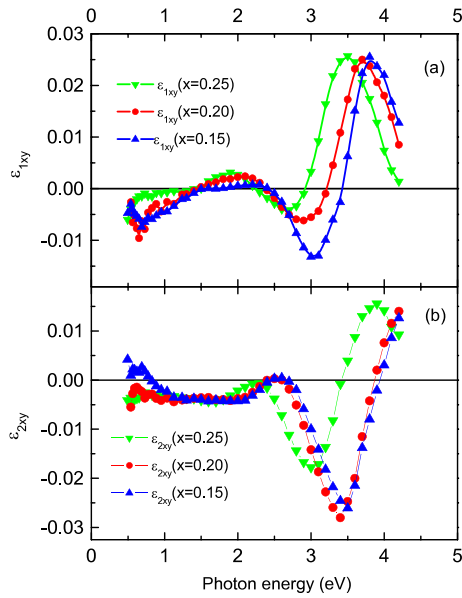


Figure 9. Energy dependence of ϵ_{1xy} (a) and ϵ_{2xy} (b) of $\text{La}_{1-x}\text{Ba}_x\text{MnO}_3$ single crystals at $T = 95$ K.

given in [39], see figure 10. This transition can be associated with allowed electro-dipole charge-transfer transition in the octahedral complex $[\text{MnO}_6]^{9-}$, see [6, 16].

The spectra of ϵ_{1xy} and ϵ_{2xy} of $\text{La}_{0.75}\text{Ba}_{0.25}\text{MnO}_3$ at $T = 300$ K (figure 10) differ significantly from the spectra taken at $T = 95$ K, which indicates that transitions responsible for the MOKE effect at these temperatures are different. A similar situation was earlier observed in a $\text{La}_{0.8}\text{Sr}_{0.2}\text{MnO}_3$ single crystal in which the ‘diamagnetic’ transition at $E = 3.5$ eV occurs only in the low temperature region while the ‘paramagnetic’ transition at $E = 3.2$ eV was found to dominate at room temperature [16].

The MOKE temperature dependence exhibits broad temperature hysteresis in the region near T_C , see the inset in figure 8. Unlike in $\text{La}_{1-x}\text{Sr}_x\text{MnO}_3$ crystals [16], in the La–Ba manganites, the annealing in Ar atmosphere did not eliminate this hysteresis completely. The Curie temperatures found from

the $\delta_p(T)$ dependence measured in the heating run are very close to T_C obtained from magnetization measurements. It is likely that the hysteresis is due to formation of ferromagnetic clusters which contribute to the magneto-optical response even in the paramagnetic range. Apparently the number and size of the clusters depends on the sample prehistory. Also the structural transition from the low temperature orthorhombic $Pnma$ phase to the high temperature $R\bar{3}c$ phase occurs not very far from T_C [27–29, 40, 41]. The structural transition gives rise to the very broad temperature hysteresis and hence may amplify the hysteretic effects in MOKE.

8. Discussion

The optical properties of the La–Ba manganites are overall similar to those of La–Sr manganites. If the photon energy is of the order or exceeds 1 eV, the optical spectra can be satisfactorily understood in terms of transitions between energy levels of the MnO_6 complex or between levels of two neighboring Mn ions. Apparently, this pure ionic approach is successful because the energy bands in the CMR manganites are known to be fairly narrow.

If the photon energy is well below 1 eV but remains greater than the energy of the phonons, the charge carriers in extended states or localized carriers that hop between randomly distributed centers dominate the optical conductivity and permittivity. In this region, a simple ionic picture is inappropriate and one needs to take into consideration the principal features of the band structure. The main question is whether there exists an energy gap or not.

Look first at figure 3, where the $\sigma_{1xx}(E, T = 95 \text{ K})$ curves are shown. The $x = 0.25$ manganite exhibits the Drude-like increase at $E \rightarrow 0$, so there is no energy gap. It was mentioned in section 4 that the $x = 0.20$ crystal is very close to the metal–semiconductor transition, therefore the energy gap in this compound is close to zero. To estimate, at least roughly, the gap in the $x = 0.15$ sample, we note that at the low-energy wings of band 1, the curves for $x = 0.15$ and 0.20 crystals are practically parallel to each other. This suggests that the difference between these two curves results

from the shift of the bottom of a high-energy band, which is just above the Fermi level, towards the valence band, whose top is just below the Fermi level. If this is the case, the gap in $\text{La}_{0.85}\text{Ba}_{0.15}\text{MnO}_3$ is about 0.15–0.20 eV. The value obtained is consistent with the width of the effective energy layer, $\varepsilon_o = 0.11$ eV, the charge carriers of which contribute to the variable range conductivity [29].

Figure 2 shows that band 1 shifts towards higher energies with increasing temperature, which indicates that the energy gap increases when the temperature rises. As the Drude-like behavior is not observed at $T = 300$ and 400 K, we may infer that in the paramagnetic state, the gap is not equal to zero in all the crystals, which agrees with previous publications on electronic transport [27–29]. Unfortunately, our data are insufficient to obtain the numerical value of the gap.

The $x = 0.25$ sample is of special interest, because in this manganite the metal–semiconductor transition takes place. We see that the transition results from (or, at least, is accompanied by) the appearance of the non-zero gap. It should be pointed out that band 1 is practically the same at $T = 300$ and 400 K, i.e. both at the Curie temperature and well above T_C . Therefore the gap vanishes and the metal–semiconductor transition occurs in the ferromagnetic state somewhat below T_C rather than at $T = T_C$, as some authors assume. This conclusion agrees with the fact that the conductivity at $T = T_C$ ($\approx 73 \Omega^{-1} \text{cm}^{-1}$) is by an order of magnitude less than the minimum metallic conductivity ($\approx 10^3 \Omega^{-1} \text{cm}^{-1}$).

Many authors discuss the possibility of polaron conductivity in the CMR manganites, see e.g. [1]. The results of section 5 conclusively indicate that the polarons contribute to the conductivity of $\text{La}_{0.85}\text{Ba}_{0.15}\text{MnO}_3$ at $T > T_C$. On the other hand, in the case of $\text{La}_{0.75}\text{Ba}_{0.25}\text{MnO}_3$, we do not find any evidence for polaron formation at $T > T_C$, although in the paramagnetic state this manganite is a semiconductor. In other words, the polarons are absent in the paramagnetic semiconductor state if, at $T \ll T_C$, a manganite is in the ferromagnetic metallic state. This conclusion seems to be quite reasonable because an increase in doping level should result in overlapping of polaron states.

The CMR effect in manganites is frequently attributed to the appearance of metallic inclusions embedded in the semiconductor matrix. There is no doubt that such inclusions indeed can exist, especially below the Curie temperature, because when the energy gap (averaged over a crystal) is small, inevitable fluctuations of the divalent concentration result in vanishing of the gap in a part of the sample. A similar situation is well known in semiconductor physics [42]. A quite different issue is, however, whether the CMR is due to the appearance of the metallic droplets. It has been obtained in section 6 that in $\text{La}_{0.85}\text{Ba}_{0.15}\text{MnO}_3$, even at $T = 190$ K, i.e. appreciably below $T_C = 214$ K, the metallic phase occupies about 1% of the total volume of the sample. Near the Curie temperature, where the maximum value of magnetoresistance is observed, see the inset in figure 1, the volume of the metallic inclusions is of course less than 1%. This small fraction of the metallic phase does not practically influence the dc resistivity.

In $\text{La}_{1-x}\text{Ba}_x\text{MnO}_3$ the values of ε_{1xy} and ε_{2xy} are essentially less and the bands are wider than in $\text{La}_{1-x}\text{Sr}_x\text{MnO}_3$

with the same x ; moreover, the Kerr effect in the La–Ba manganite is observed even in the paramagnetic phase. Thus in La–Ba crystals the magnetic and charge inhomogeneity is stronger than in La–Sr ones.

9. Conclusions

The optical spectra of ferromagnetic $\text{La}_{1-x}\text{Ba}_x\text{MnO}_3$ single crystals have been found to be similar to those of $\text{La}_{1-x}\text{Sr}_x\text{MnO}_3$, both in the ferromagnetic and paramagnetic states. If the photon energy is of the order or exceeds 1 eV, the optical spectra can be satisfactorily understood in terms of transitions between energy levels of the MnO_6 complex or between levels of two neighboring Mn ions.

At $T \ll T_C$ the energy gap in the $\text{La}_{0.85}\text{Ba}_{0.15}\text{MnO}_3$ is about 0.15–0.20 eV, the gap in the $\text{La}_{0.80}\text{Ba}_{0.20}\text{MnO}_3$ is close to zero, and in the $\text{La}_{0.75}\text{Ba}_{0.25}\text{MnO}_3$ it is absent. Well above the Curie temperature the energy gap is not equal to zero in all the crystals. The $x = 0.25$ manganite undergoes a transition from the metallic state to the semiconductor one somewhat below T_C rather than at $T = T_C$.

In the paramagnetic state the polarons have been found to contribute to the conductivity of $\text{La}_{0.85}\text{Ba}_{0.15}\text{MnO}_3$ and perhaps of $\text{La}_{0.80}\text{Ba}_{0.20}\text{MnO}_3$ single crystals.

The volume of the metallic inclusions has been estimated in $\text{La}_{0.85}\text{Ba}_{0.15}\text{MnO}_3$ at the temperature which is appreciably below T_C . It has been obtained that the metallic phase occupies about 1% of the total volume of the sample. This small fraction of the metallic phase does not practically influence the dc resistivity.

In La–Ba manganites the spectra of ε_{xy} depend noticeably on the divalent ion content. At $E > 2.5$ eV the strong magneto-optical effect is likely to be due mainly to a ‘diamagnetic’ transition at $E \approx 3.5$ eV. The magnetic and charge inhomogeneity in the $\text{La}_{1-x}\text{Ba}_x\text{MnO}_3$ single crystals is stronger than in the $\text{La}_{1-x}\text{Sr}_x\text{MnO}_3$ ones.

Acknowledgments

This work was supported by the RFBR (grants 09-02-00081 and 06-02-16085) and Program No.5 of the Presidium of RAS.

References

- [1] Salamon M B and Jaime M 2001 *Rev. Mod. Phys.* **73** 583
- [2] Dagotto E 2002 *Nanoscale Phase Separation and Colossal Magnetoresistance. The Physics of Manganites and Related Compounds* (Berlin: Springer)
- [3] Ziese M 2002 *Rep. Prog. Phys.* **65** 143
- [4] Haghiri-Gosnet A-M and Renard J-P 2003 *J. Phys. D: Appl. Phys.* **36** R127
- [5] Tokura Y 2006 *Rep. Prog. Phys.* **69** 797
- [6] Gan'shina E, Loshkareva N, Sukhorukov Yu, Mostovshchikova E, Vinogradov A and Nomerovannaya L 2006 *J. Magn. Magn. Mater.* **300** 62
- [7] Kovaleva N N, Boris A V, Bernhard C, Kulakov A, Pimenov A, Balbashov A M, Khaliullin G and Keimer B 2004 *Phys. Rev. Lett.* **93** 147204
- [8] Moskvin A S 2002 *Phys. Rev. B* **65** 205113
- [9] Moskvin A S 2009 *Phys. Rev. B* **79** 115102

- [10] Loshkareva N N, Sukhorukov Yu P, Mostovshchikova E V, Nomerovannaya L V, Makhnev A A, Naumov S V, Gan'shina E A, Rodin I K, Moskvina A S and Balbashov A M 2002 *JETP* **94** 350
- [11] Okimoto Y, Katsufuji T, Ishikawa T, Arima T and Tokura Y 1997 *Phys. Rev. B* **55** 4206
- [12] Takenaka K, Iida K, Sawaki Y, Sugai S, Moritomo Y and Nakamura A 1999 *Phys. Status Solidi b* **215** 637
- [13] Takenaka K, Sawaki Y and Sugai S 1999 *Phys. Rev. B* **60** 13011
- [14] Takenaka K, Shiozaki R and Sugai S 2002 *Phys. Rev. B* **65** 184436
- [15] Yamaguchi S, Okimoto Y, Ishibashi K and Tokura Y 1998 *Phys. Rev. B* **58** 6862
- [16] Gan'shina E A, Vashuk M V, Vinogradov A N and Mukovskii Ya M 2006 *J. Magn. Magn. Mater.* **300** e126
- [17] Okuda T, Tomioka Y, Asamitsu A and Tokura Y 2000 *Phys. Rev. B* **61** 8009
- [18] Zainullina R I, Bebenin N G, Ustinov V V, Mukovskii Ya M and Shulyatev D A 2007 *Phys. Rev. B* **76** 014408
- [19] Boris A V, Kovaleva N N, Bazhenov A V, van Bentum P J M, Rasing Th, Cheong S-W, Samoilov A V and Yeh N-C 1999 *Phys. Rev. B* **59** R697
- [20] Kim K H, Jung J H and Noh T W 1998 *Phys. Rev. Lett.* **81** 1517
- [21] Quijada M A, Černe J, Simpson J R, Drew H D, Ahn K H, Millis A J, Shreekala R, Ramesh R, Rajeswari M and Venkatesan T 1998 *Phys. Rev. B* **58** 16093
- [22] Sacchetti A, Döre P, Postorino P and Congeduti A 2004 *J. Phys. Chem. Solids* **65** 1431
- [23] Rauer R, Rübhausen M and Dörr K 2006 *Phys. Rev. B* **73** 092402
- [24] Rusydi A, Rauer R, Neuber G, Bastjan M, Mahns I, Müller S, Saichu P, Schulz B, Singer S G, Lichtenstein A I, Qi D, Gao X, Yu X, Wee A T S, Stryganyuk G, Dörr K, Sawatzky G A, Cooper S L and Rübhausen M 2008 *Phys. Rev. B* **78** 125110
- [25] Sukhorukov Yu P, Gan'shina E A, Belevtsev B I, Loshkareva N N, Vinogradov A N, Rathnayaka K D D, Parasiris A and Naugle D G 2002 *J. Appl. Phys.* **91** 4403
- [26] Roy C and Budhani R C 1999 *J. Appl. Phys.* **83** 3124
- [27] Bebenin N G, Zainullina R I, Mashkautsan V V, Gaviko V S, Ustinov V V, Mukovskii Ya M and Shulyatev D A 2000 *JETP* **90** 1027
- [28] Zainullina R I, Bebenin N G, Mashkautsan V V, Ustinov V V, Mukovskii Ya M and Arsenov A A 2003 *Phys. Status Solidi* **45** 1754
- [29] Bebenin N G, Zainullina R I, Chusheva N S, Ustinov V V and Mukovskii Ya M 2005 *J. Phys.: Condens. Matter* **17** 5433
- [30] Shulyatev D, Kozlovskaya N, Privezentsev R, Pestun A, Mukovskii Ya, Elochina L and Zverkov S 2006 *J. Cryst. Growth* **291** 262
- [31] Laukhin V, Martínez B, Fontcuberta J and Mukovskii Y M 2001 *Phys. Rev. B* **63** 214417
- [32] Krinchik G S 1985 *Physics of Magnetic Phenomena* (Moscow: Lomonosov MSU) (in Russian)
- [33] Jung J H, Kim K H, Lee H J, Ahn J S, Hur N J, Noh T W, Kim M S and Park J-G 1999 *Phys. Rev. B* **59** 3793
- [34] Klinger M I and Samokhvalov A A 1977 *Phys. Status Solidi b* **79** 9
- [35] Gerthsen P, Groth R, Hardtl K H, Heese D and Reik H D 1965 *Solid State Commun.* **3** 165
- [36] Reik H G, Kauer E and Gerthsen P 1964 *Phys. Lett.* **8** 29
- [37] Emin D 1975 *Adv. Phys.* **24** 305
- [38] Mostovshchikova E V, Bebenin N G and Loshkareva N N 2004 *Phys. Rev. B* **70** 012406
- [39] Suits J C 1972 *IEEE Trans. Magn.* **8** 95
- [40] Zainullina R I, Bebenin N G, Burkhanov A M, Ustinov V V and Mukovskii Ya M 2005 *J. Alloys Compounds* **394** 39
- [41] Gaviko V S, Bebenin N G and Mukovskii Ya M 2008 *Phys. Rev. B* **77** 224105
- [42] Shklovskii B I and Efros A L 1984 *Electronic Properties of Doped Semiconductors* (*Springer Series in Solid-State Sciences* vol 45) (Berlin: Springer)